

Article

Micro-Structure and Thermomechanical Properties of Crosslinked Epoxy Composite Modified by Nano-SiO₂: A Molecular Dynamics Simulation

Qing Xie ^{1,*}, Kexin Fu ¹ , Shaodong Liang ¹ , Bowen Liu ¹, Lu Lu ¹, Xueming Yang ², Zhengyong Huang ³ and Fangcheng Lü ¹

¹ State Key Laboratory of Alternate Electrical Power System with Renewable Energy Sources, North China Electric Power University, Baoding 071000, China; fku_ncepu@foxmail.com (K.F.); liangshao9564@163.com (S.L.); bowensmz@hotmail.com (B.L.); andrewlu149@163.com (L.L.); 13582251628@126.com (F.L.)

² Department of Power Engineering, North China Electric Power University, Baoding 071003, China; yxmhhx@163.com

³ State Key Laboratory of Power Transmission Equipment & System Security and New Technology, Chongqing University, Chongqing 400044, China; huangzhengyong@cqu.edu.cn

* Correspondence: xq_ncepu@126.com; Tel.: +86-0312-7522-767

Received: 3 July 2018; Accepted: 19 July 2018; Published: 20 July 2018



Abstract: Establishing the relationship among the composition, structure and property of the associated materials at the molecular level is of great significance to the rational design of high-performance electrical insulating Epoxy Resin (EP) and its composites. In this paper, the molecular models of pure Diglycidyl Ether of Bisphenol A resin/Methyltetrahydrophthalic Anhydride (DGEBA/MTHPA) and their nanocomposites containing nano-SiO₂ with different particle sizes were constructed. The effects of nano-SiO₂ dopants and the crosslinked structure on the micro-structure and thermomechanical properties were investigated using molecular dynamics simulations. The results show that the increase of crosslinking density enhances the thermal and mechanical properties of pure EP and EP nanocomposites. In addition, doping nano-SiO₂ particles into EP can effectively improve the properties, as well, and the effectiveness is closely related to the particle size of nano-SiO₂. Moreover, the results indicate that the glass transition temperature (T_g) value increases with the decreasing particle size. Compared with pure EP, the T_g value of the 6.5 Å composite model increases by 6.68%. On the contrary, the variation of the Coefficient of Thermal Expansion (CTE) in the glassy state demonstrates the opposite trend compared with T_g . The CTE of the 10 Å composite model is the lowest, which is 7.70% less than that of pure EP. The mechanical properties first increase and then decrease with the decreasing particle size. Both the Young's modulus and shear modulus reach the maximum value at 7.6 Å, with noticeable increases by 12.60% and 8.72%, respectively compared to the pure EP. In addition, the thermal and mechanical properties are closely related to the Fraction of Free Volume (FFV) and Mean Squared Displacement (MSD). The crosslinking process and the nano-SiO₂ doping reduce the FFV and MSD value in the model, resulting in better thermal and mechanical properties.

Keywords: epoxy resin composites; nano-SiO₂; molecular dynamics; crosslinked structure; free volume; segment motion; glass transition temperature; coefficient of thermal expansion; mechanical properties

1. Introduction

With the growing expansion of electrical equipment applications, the disadvantages of the Epoxy Resin (EP) insulating materials such as Diglycidyl Ether of Bisphenol A resin/Methyltetrahydrophthalic Anhydride (DGEBA/MTHPA) have become increasingly obvious. Some of the properties, including

mechanical and thermal properties, are often not able to meet the ever-increasing requirements of electrical equipment [1–4]; while, the emergence of nanomaterials and the development of nanotechnology in recent years have provided new ways to improve the comprehensive properties of EP [5,6]. Compared with traditional materials, the distinguishing structure of nanomaterial has provided a set of unique features, such as the small size effect, quantum size effect and surface effect [7,8], which further enhance the performance in various aspects of physics and chemistry. The nanocomposites obtained by combining the nanofillers with the polymer possess the advantages of both the nanomaterial and the polymer itself. Numerous scholars have carried out experimental studies on the improvement of EP thermal properties, mechanical properties, electrical properties, etc. [9,10]. The studies emphasized the effects of filler type, particle size, shape and dosage on the properties of the composite EP [11,12]. Despite the progress made by the above researchers, there is no unified understanding of the interface mechanism of EP nanocomposites. Therefore, it is significant to further conduct research on the relationship between the structure and properties of EP nanocomposite, as well as investigating the underlying mechanism of action.

In recent years, molecular simulation technologies have continued to progress and develop, which, at the molecular level, possess obvious advantages in the study of the microstructure and macro-properties of composite polymer materials [13–15]. In particular, the Molecular Dynamics (MD) method has been applied to the study of EP by various scholars [16–20]. In terms of EP composites, some scholars have studied the glass transition and thermoelasticity of SiC/EP nanocomposites by molecular simulation. It is found that the glass transition temperature (T_g) and the Coefficient of Thermal Expansion (CTE) of the composites is lower than that of the pure EP [21]. Chen Shenghui et al. [22] have constructed an uncrosslinked DGEBA and Isophorone Diamine (DGEBA/IPD) epoxy-carbon nanofiber composite interface model, analyzed the distribution, structure and movement characteristics of the monomer molecules and found that carbon nanofibers can significantly alter the concentration and properties of the EP and curing agent during the interfacial phase. Zhang et al. [20] investigated the influence of silane coupling agent on the structure and thermomechanical properties of the nanocomposites through MD simulation and found that incorporating silica nanoparticles into the EP matrix can significantly improve the mechanical and thermal properties of the composites. Furthermore, the thermomechanical properties were further enhanced by silane coupling agent modification on the surface of fillers. R. Zhu et al. [23] carried out MD research on EPON-862 EP (Bisphenol F epoxy resin) reinforced by the carbon nanotube. It was found that the carbon nanotubes can enhance the mechanical properties of the EP. Moreover, with the increase of the aspect ratio, the enhancement effect is more significant. In summary, MD has become an essential instrument in terms of analyzing the performance of composite materials, which is also expected to provide new approaches for the design and preparation of EP composites with enhanced performance.

SiO₂ is one of the most common fillers for the EP insulating materials. The EP composite filled with nano-SiO₂ has improved mechanical and thermal properties [7,24,25]. Although scholars have studied the properties of SiO₂/EP nanocomposites through experiments [26–30], few involved MD simulations.

In this paper, MD simulations were performed on DGEBA/MTHPA EP filled with nano-SiO₂. The SiO₂ fillers were spherical, with particle radiuses of 6.5 Å, 7.6 Å, 8.8 Å and 10 Å, respectively. Based on the MD simulations, the parameters of the models, including the Fraction of Free Volume (FFV), Mean Square Displacement (MSD), T_g , CTE and mechanical properties, were analyzed. The effects of crosslinking density and nano-SiO₂ particle size on the microstructure, thermal and mechanical properties of EP were investigated. In addition, the relationship between the structure and properties of composite EP was analyzed. Furthermore, this paper provided theoretical guidance for the design and preparation of EP nanocomposites with enhanced performance.

2. Model Construction and Simulation Details

In this section, the simulation steps are synthesized as the following three parts: (1) mix DGEBA and MTHPA according to the actual proportion, and fill the models with nano-SiO₂; (2) construct the amorphous models of the crosslinked EP/SiO₂ nanocomposites based on the practical crosslinking reaction mechanism; (3) perform MD simulations of DGEBA/MTHPA/SiO₂ crosslinked models with

different crosslinking densities and filler sizes. The models mentioned in this paper were built using Material Studio (developed by Accelrys).

2.1. Reaction Mechanism of EP and Curing Agent

Due to the existence of the numerous hydroxyl groups on the surface of nano-SiO₂, nanofillers were also considered during the crosslinking reaction. The reaction mechanism is shown in Figure 1. By repeating the process in Figure 1c,d, the crosslinking reaction was carried out.

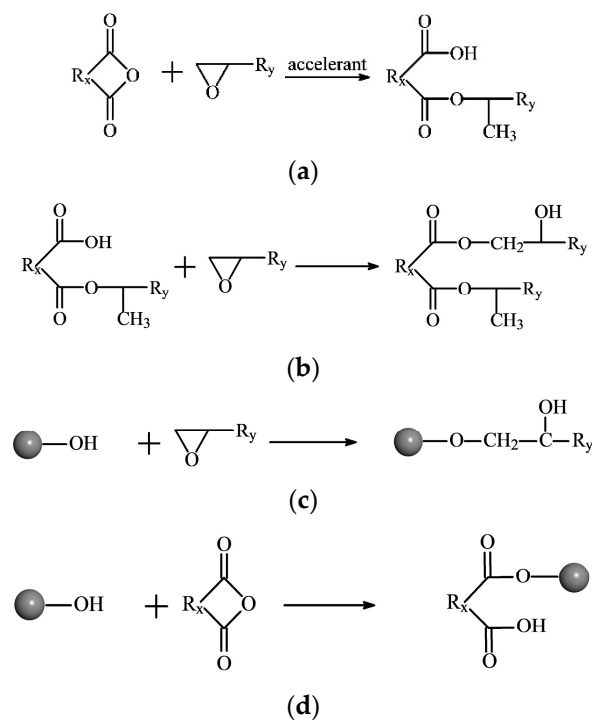


Figure 1. Mechanism of crosslinking reaction between the epoxy, acid anhydride curing agent and nano-SiO₂. (a) Under the effect of trace moisture existing in the system, part of the epoxy groups open and anhydrides hydrolyze to further react with each other and produce monoester containing carboxyl; (b) carboxyl reacts with the epoxy groups and generates hydroxyl groups; (c) the hydroxyl groups on the surface of SiO₂ and the generated hydroxyl react with the epoxy groups to generate hydroxyl groups; (d) the hydroxyl groups on the surface of SiO₂ and the generated hydroxyl react with anhydrides to generate carboxylic acids.

Here, the crosslinking reaction between DGEBA, MTHPA and SiO₂ was realized through programming. To simplify the process, the following assumptions have been made: (1) The crosslinking density is defined as the ratio of the reacted epoxy groups to the initial epoxy groups. (2) To start the crosslinking process, we introduce the partial product of (a) during the model construction stage (i.e., ignoring Reaction (a) in the crosslinking process) as a crosslinking primer (denoted by DGEBA-MTHPA). As a result, the crosslinking density of the initial model is 10%. (3) The activity of each reaction group is the same. (4) The reaction is diffusion controlled. (5) The reactions are synchronized.

2.2. Construction of Crosslinked EP/SiO₂ Composite Models

Epoxy prepolymer is regarded as a mixture of DGEBA with a polymerization degree of zero and one. In this paper, the polymerization degree of DGEBA was set to zero in the modeling process to simplify the composite model [23]. The modeling process of crosslinked EP/SiO₂ composite is as follows:

- (1) Construct the molecular models of DGEBA, MTHPA, DGEBA-MTHPA and spherical nano-SiO₂ with radiuses of 6.5 Å, 7.6 Å, 8.8 Å and 10 Å, respectively. Simulate the oxidation reaction of SiO₂, so that the surface of fillers has massive hydroxyl groups [31,32]. Subsequently, optimize the structure of the above models and obtain the molecular models as shown in Figure 2.
- (2) Considering that the actual molar ratio of DGEBA and MTHPA is about 1:2 [20,33], we constructed amorphous molecular models of pure EP and EP nanocomposite with different filler sizes. Using periodic boundary conditions, the initial temperature of the model was set to be 580 K to facilitate the subsequent annealing process. Each nanocomposite model was filled with a nano-SiO₂ particle to simulate the well-dispersed situation. The mass fraction of SiO₂ in each system was maintained at 6.5% by adjusting the amount of the ingredients according to Table 1. Further, 10 amorphous molecular models with an initial crosslinking density of 10% were constructed under each system, and their geometric structures were optimized based on the minimum energy principle. The amorphous models with the lowest energy were selected for further simulation and calculation.
- (3) Perform a 200-ps MD simulation on each model under the NPT ensemble (the constant temperature and pressure ensemble). The specific details of the MD process are as follows. The time step was 1 fs. The temperature and pressure were controlled at 580 K and 1.0×10^{-4} GPa (which is one standard atmospheric pressure) respectively by applying the Andersen and Berendsen methodology [20,34]. In addition, the van der Waals interaction and electrostatic interaction were calculated by the atom-based and Eward method, respectively.
- (4) The scriptlet employed for the crosslinking reaction was written according to Section 2.1. The crosslinking was conducted in stages, and the molecular models with different crosslinking densities were obtained by conducting crosslinking reactions multiple times.

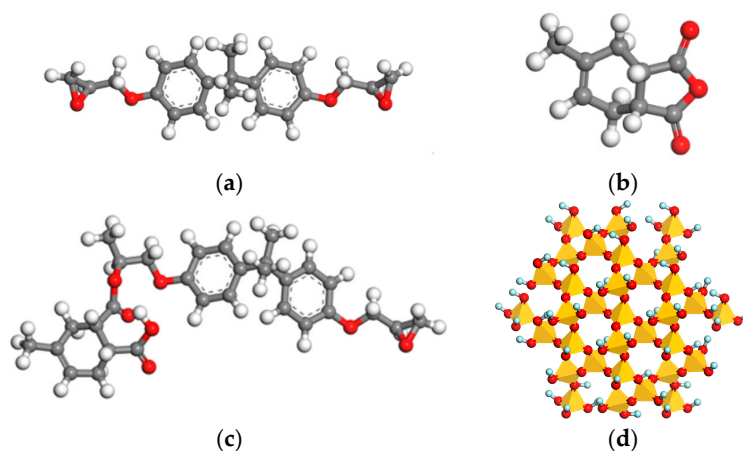


Figure 2. Molecular models. (a) Diglycidyl Ether of Bisphenol A resin (DGEBA); (b) Methyltetrahydrophthalic Anhydride (MTHPA); (c) DGEBA-MTHPA; (d) SiO₂.

Table 1. Initial components of the molecular model of each system.

Particle Size of SiO ₂ (Å)	Molecular Number of			Atomic Number
	DGEBA	MTHPA	DGEBA-MTHPA	
none	40	90	10	4650
6.5	40	90	10	4838
7.6	65	146	16	7823
8.8	88	199	23	10,708
10	124	288	40	15,830

2.3. MD and Annealing Simulation

Molecular models with crosslinking densities of 10%, 34%, 67% and 96% were further selected for MD processing. First, MD simulations of 200 ps were performed under the NVT ensemble (constant volume and temperature ensemble) and NPT ensemble successively, in order to eliminate the stress generated during the crosslinking process. The time step was 1 fs, and the temperature was 580 K. In addition, the pressure in the NPT ensemble was controlled at 1.0×10^{-4} GPa.

Subsequently, anneal simulations were performed on the above models from 580 K–280 K to extract the information of density, volume and temperature for thermal property analysis. The annealing rate was set to be 10 K/100 ps, i.e., an NPT ensemble MD simulation of 100 ps was performed after each temperature decrease by 10 K. The models of EP composite at 300 K are shown in Figure 3.

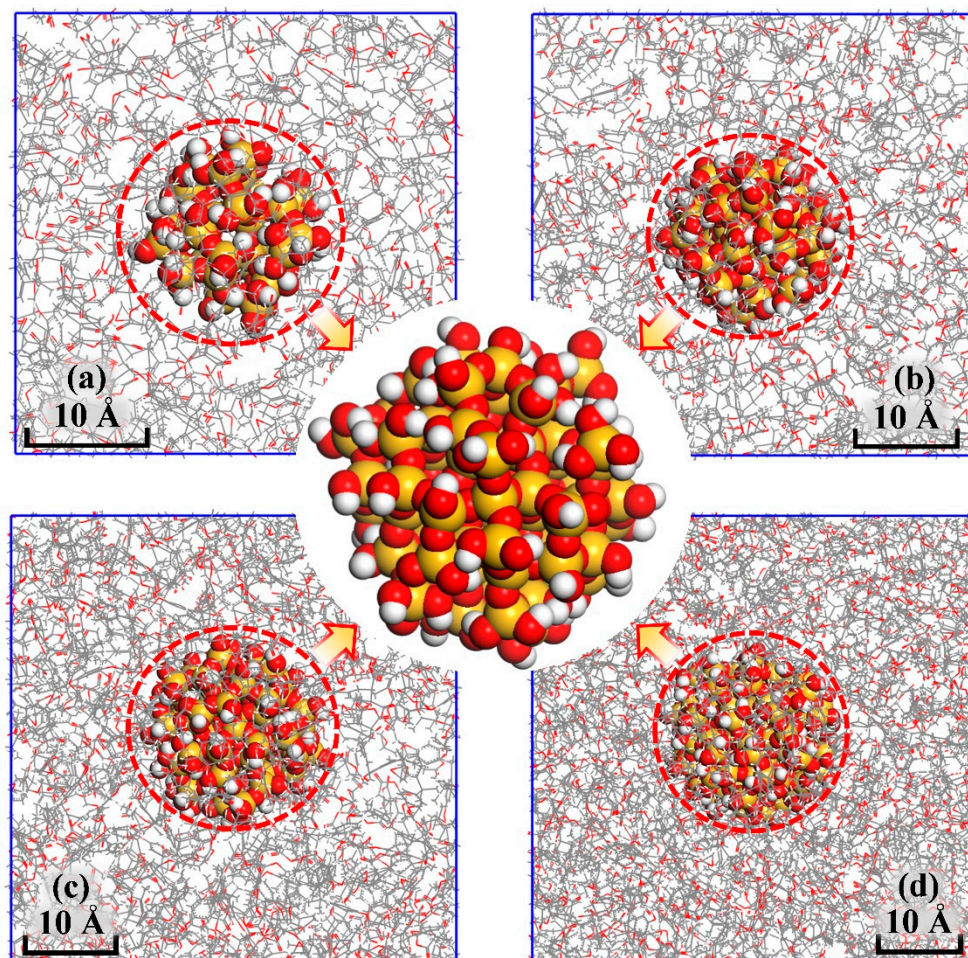


Figure 3. The crosslinked network in Epoxy Resin (EP) nanocomposite models. (a) For 6.5 Å; (b) for 7.6 Å; (c) for 8.8 Å; (d) for 10 Å.

3. Simulation Results and Model Parameters

3.1. Free Volume

The free volume theory [35] holds that the volume of a liquid or solid substance, V_T , consists of two parts, i.e., the volume occupied by the molecule denoted as V_o , and the free volume V_f , where:

$$V_T = V_o + V_f \quad (1)$$

V_f is the intermolecular space, which disperses in the form of a hole among the materials and provides space for molecule movements. It also enables the movement of the molecular chain. The influence of nanoparticles on the free volume of the polymer was relatively complex in the following two aspects. First, the nanoparticle occupied a considerable part of the volume of the system and increased the distance between chain segments, which hindered the movement and stacking of molecular segments and reduced the free volume. Moreover, the nanoparticle can participate in the crosslinking reaction of the EP system and fix molecular chain segments, therefore expanding the crosslinked network and increasing the free volume. The above impacts existed in all the EP nanocomposite materials. Therefore, the increase or decrease of the free volume significantly depended on the properties of the nanoparticles.

The volumes of different models differed greatly due to the different numbers of molecules. As a result, the free volumes were different, as well. Therefore, to facilitate the comparison of the free volume characteristics of different systems, the fraction of free volume (*FFV*) was introduced to characterize the relative size of the free volume. The expression is [35]:

$$FFV = \frac{V_f}{V_0 + V_f} \times 100\% \quad (2)$$

Here, the *FFV* of EP/nano-SiO₂ composites with different particle sizes were calculated at 300 K. The variation trend of the *FFV* with the crosslinking density is shown in Figure 4.

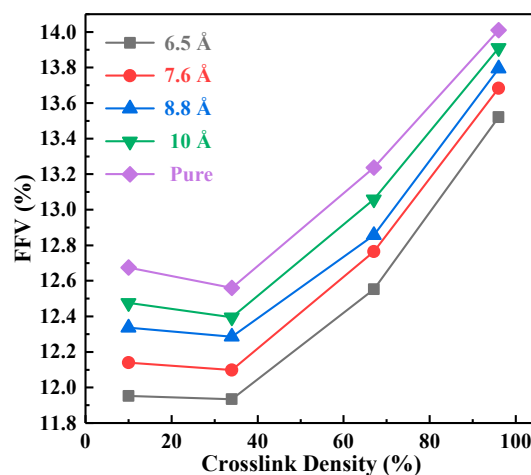


Figure 4. The Fraction of Free Volume (*FFV*) of each system with different crosslinking densities.

According to Figure 4, with the increase of crosslinking density, the *FFVs* of pure EP and composites decrease first and then increased. The reason for the above trend is as follows. In the initial stage of the crosslinking reaction, the free volume in the crosslinking network was occupied by a dangling chain appearing [36,37]; therefore, the *FFV* of the system decreased slightly. Subsequently, the formation of a crosslinking network and the decrease of the dangling segment led to the increase of the free volume. On the other hand, the *FFV* of the nanocomposites was lower than that of the pure EP. The underlying cause is that the nanoparticles occupied a considerable part of the space in the system, resulting in a smaller range of segmental motion and a decrease in the *FFV*. Furthermore, the *FFV* decreased with the decreasing particle size. This was due to the final crosslinked network being generated by the covalent links between SiO₂ and EP matrix in the system, and the interaction tended to enhance as the particle size decreased. Previous studies have suggested that the mechanical properties of the polymers depended on the free volume to a certain extent. The smaller the free volume was, the better the performance could be [35,38]. Therefore, it can be inferred that the mechanical properties of the system containing fillers were better than that of the pure EP system. Moreover, the smaller the particle size was, the better the mechanical property was when the crosslinking density was relatively high.

3.2. Segment Motion

The molecules of the models were constantly moving throughout the MD process. Some research has proven that there is a correlation between the strength of the segment motion and the mechanical properties of the polymer. Specifically, the enhancement of molecular segment motion may reduce the mechanical modulus of EP [39]. Moreover, the mean squared displacement (*MSD*) is defined as a microscopic parameter to characterize the motion capability of each atom or molecular segment in the system, which is defined as the mean squared displacement of the molecules or segments, respectively. In general, the slope of the *MSD* curve indicates the strength of the polymer molecule segment motion. The *MSD* in a system containing *N* atoms can be described as follows [38]:

$$MSD = \frac{1}{3N} \sum_{i=0}^{N-1} \left[\left| \vec{R}_i(t) - \vec{R}_i(0) \right|^2 \right] \tag{3}$$

where $\vec{R}_i(t)$ and $\vec{R}_i(0)$ denote the displacement vector of any atom *i* at time *t* and the initial time in the system, respectively. In this paper, the *MSD* values of systems with different crosslinking densities, particle sizes and temperature in the first 30 ps of MD simulations under the NPT ensemble were investigated.

The *MSD* values of the 6.5 Å system under different crosslinking densities are shown in Figure 5a. In addition, the trends of *MSD* and crosslinking density in other systems were similar. As the crosslinking density increased, the *MSD* values of EP and its nanocomposites gradually decreased, which indicated that the crosslinked structure limited the molecular motion in the model. To analyze the effect of particle size on the segment motion, the *MSD* values of different particle size models were normalized based on the number of atoms in the pure EP system, as suggested in Table 1. The processed *MSD* values are shown in Figure 5c. The segment motion was negatively correlated with the particle size. It can be seen that nano-SiO₂ dopants can significantly limit the movement of the molecular segment in the material, and the restriction will be more pronounced as the particle size increases. In addition, temperature had a significant effect on segmental motion. Particularly, temperature had an apparent effect on the segmental motion of EP and its composites, as well. With the increasing of temperature, *MSD* values increased continuously, as shown in Figure 5b. This tendency was due to the thermal motion of the molecules. As the temperature increased, the thermal motion of the molecule increased, which caused the increasing of *MSD*. Furthermore, in the temperature range of 400 K–410 K, the variation of *MSD* values was the most conspicuous, which was related to the glass transition of the materials.

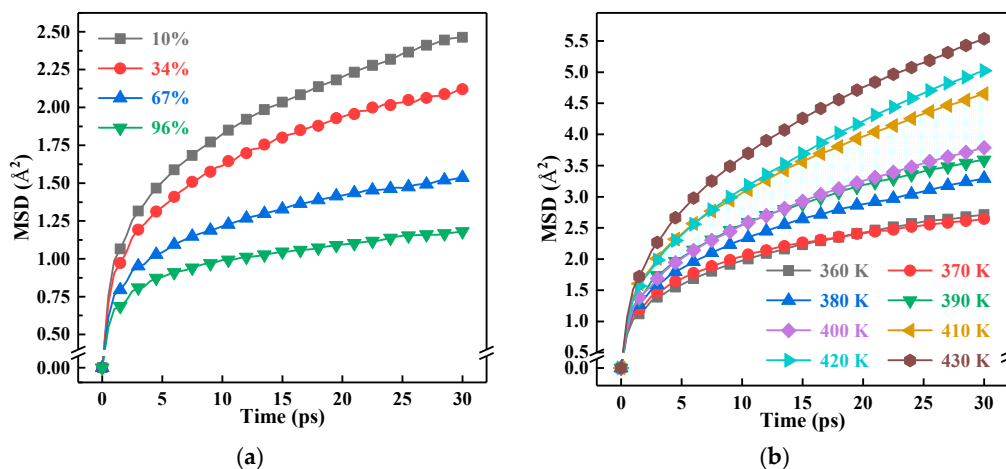


Figure 5. Cont.

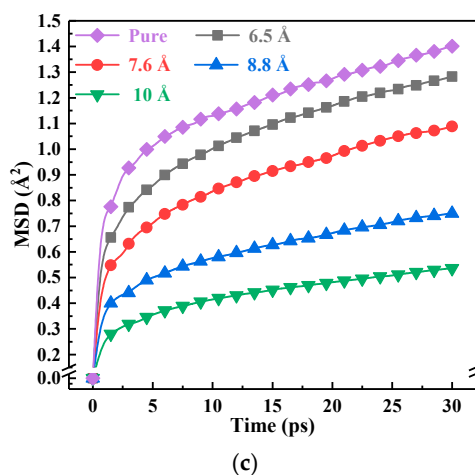


Figure 5. The variation of Mean Squared Displacement (MSD) values with time. (a) MSD values of the 6.5 Å system at 300 K with different crosslinking densities; (b) MSD values of the 67% crosslinking density system with 6.5 Å particle sizes at different temperatures; (c) MSD values of the 67% crosslinking density system at 300 K with different particle sizes.

3.3. Glass Transition Temperature

The glass transition temperature (T_g) refers to the temperature for the transition from the glassy state to the rubbery state of the amorphous polymer or vice versa, which is a critical thermal performance index of EP materials. When EP transitions from the glassy state to the rubbery state at temperature T_g , its performance completely changes due to the state conversion. Therefore, obtaining the accurate value of T_g is an important prerequisite for thermal performance comparisons across different systems. In this paper, the density-temperature linear fitting and MSD curve method were used to accurately predict the T_g of each system.

1. Density-temperature linear fitting method:

As the temperature increased, the density of the EP showed a linear decrease. However, the density decrease rates in the glassy and rubbery state were different [40,41]. We plotted the density-temperature scatter diagram based on the temperature and density extracted during the annealing process. Figure 6 presents the density-temperature curve of the 67% crosslinked pure EP, where there is an obvious inflection point in each scatter plot. The scatter points on the two sides of the inflection point are linearly fitted, and the turning point of the two lines is the T_g value of the material.

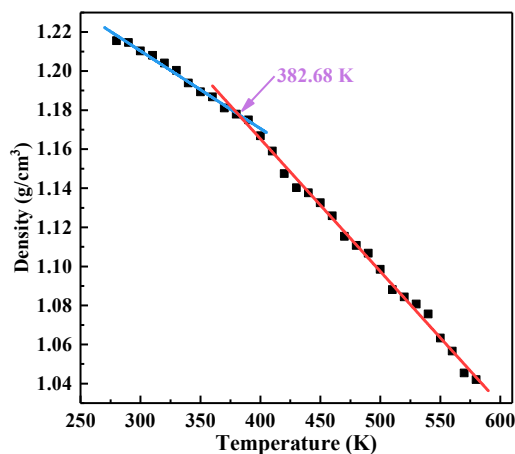


Figure 6. Linear fitting of the density-temperature curve in each system.

2. MSD curve method:

Studies have shown that as the temperature increases, the MSD gradually increases. When transitioning from the glassy state to the rubbery state, the motion state of the molecules in the system will change drastically. This mutation reflecting on the MSD curve was a sudden jump of the MSD values at the temperature interval above and lower than T_g . Therefore, by investigating the MSD characteristics of the polymers at different temperatures and observing the temperature range of these curves, the temperature range of T_g can be predicted [42].

The MSD of the pure EP and EP nanocomposite systems at various temperatures was calculated at 67% crosslinking density. To stimulate the process, the temperature interval in this paper was set to be 10 K. As shown in Figure 5b, taking the 6.5 Å EP composite system as an example, there was a wider gap between the 400 K and 410 K MSD curves. Therefore, we concluded that the T_g value of the 6.5 Å EP composite system was in the (400 K, 410 K) interval.

T_g values obtained by the density-temperature linear fitting method and the T_g intervals obtained by the MSD curve method are summarized in Table 2. The results of the two methods were highly consistent with each other. In addition, the T_g value of the pure EP with 67% crosslinking density was 382.68 K, which was highly close to the actual T_g value of DGEBA/MTHPA epoxy [43]. It can be assumed that 67% was close to the industrial crosslinking density of the pure DGEBA/MTHPA system.

Table 2. T_g value of 67% crosslink density.

Particle Size (Å)	T_g by Fitting Method (K)	T_g by MSD Curve Method (K)
6.5	408.23	400–410
7.6	397.55	390–400
8.8	395.93	390–400
10	387.39	380–390
Pure	382.68	380–390

The T_g values of EP and its composites for different particle sizes and crosslinking densities are summarized in Figure 7. According to Figure 7a, the T_g value of pure EP and EP composite with 6.5 Å nano-SiO₂ increased as the crosslinking reaction went on. Moreover, when the crosslinking density was greater than 34%, the increase rate of the T_g value with crosslinking density was higher than that in the initial stage of the crosslinking process. Therefore, increasing the crosslinking density can significantly improve the T_g value of EP and its composites. According to Figure 5a, the segmental motion in the model was limited by the crosslinked structure, and the flexibility of segments decreased. Therefore, it is difficult to alter the conformation of the models. The higher the crosslinking density, the stronger the effect was and, ultimately, the higher the T_g value.

Figure 7b shows the T_g value of pure EP and EP composite with different particle sizes at 67% crosslinking density. Nano-SiO₂ can significantly improve the T_g value of EP composites. Particularly, the T_g value of composites doped with 6.5 Å SiO₂ increased by 6.68%. Analysis suggested that the excellent thermal properties of nano-SiO₂ can increase the T_g value of the composites. On the other hand, the inorganic-organic interface integration between the filler and the EP matrix was an important factor to increase the T_g value of the material. With the decrease of the particle size, the small size effect of nanoparticles was more intense, and the interface effect was strengthened. Therefore, the interfacial bonding between the nano-SiO₂ and the matrix was stronger, resulting in higher T_g values.

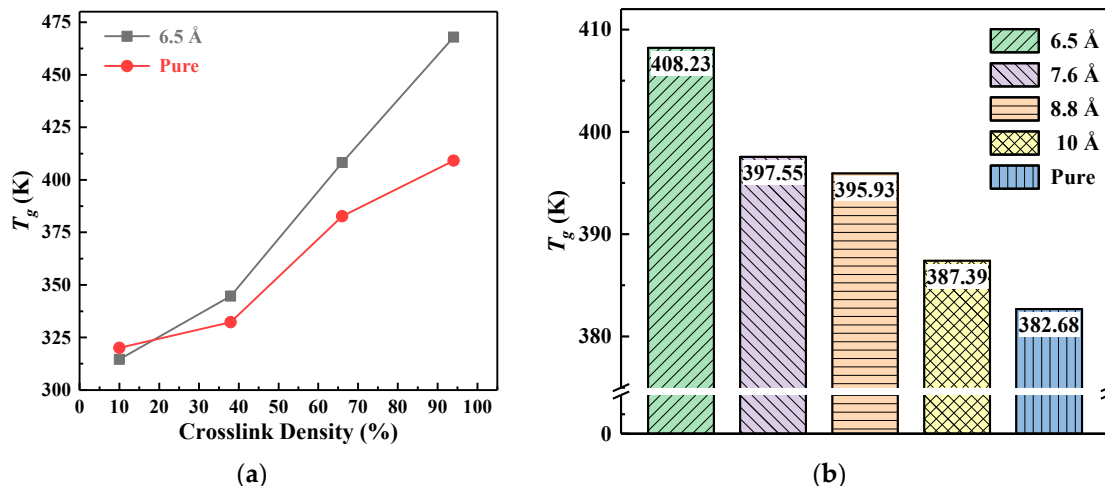


Figure 7. The T_g value of EP and its composites. (a) The T_g value of pure EP and EP composite with 6.5 Å nano-SiO₂ at different crosslinking densities; (b) the T_g value of pure EP and EP composite with different particle sizes at 67% crosslinking density.

3.4. Coefficient of Thermal Expansion

Coefficient of Thermal Expansion (CTE) refers to the ratio of the increment in the length of the unit temperature and its length at 300 K, which is a critical index factor to measure the thermal stability of materials. The calculation formula is as follows [21]:

$$CTE = \frac{1}{V_0} \left(\frac{\partial V}{\partial T} \right)_P \tag{4}$$

where V_0 is the volume at 300 K and P is taken as the standard atmospheric pressure. The relationship between the volume and temperature of different EP systems was linearly fitted to obtain the values of $\partial V / \partial T$.

Taking pure EP and the 6.5 Å composite as examples, the CTE at the glassy state and rubbery state obtained by Equation (4) are shown in Figure 8. According to Figure 8, the CTE of the two states decreased significantly with the increase of the crosslinking density. Specifically, when the crosslinking density increased from 10%–96%, the CTE of pure EP and the 6.5 Å composites in the glassy state decreased by 16.95% and 16.99%, respectively. Correspondingly, those in the rubber state decreased by 27.22% and 32.97%. This was attributed to the 3D network structure formed in the models during the crosslinking reaction, resulting in a reduced flexibility of the molecular chain and bound motion of polymer segments. However, the CTE of EP composites was lower than that of pure EP because of the extremely low CTE of the SiO₂ crystal itself. In addition, the CTE in the glassy state was smaller than that in the rubbery state due to the different states of free volume, which is consistent with [20,21,32]. In the glassy state, the free volume of the materials was in the frozen state, and the expansion of the occupied volume was the only dominant factor affecting CTE; while, in the rubbery state, both the free volume and the occupied volume contributed to the thermal expansion, which led to the higher CTE in the glassy state.

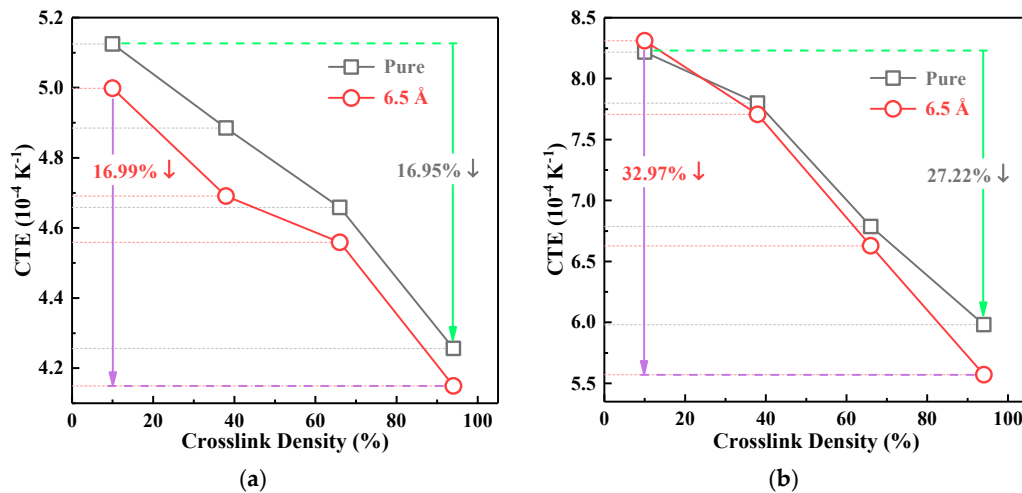


Figure 8. The Coefficient of Thermal Expansion (CTE) in the glassy state and rubbery state. (a) Glassy state; (b) rubbery state.

On the other hand, the CTE in the glassy and rubbery states showed different trends with the variation of the particle size. As shown in Figure 9, with the increase of the particle size of nano-SiO₂, the CTE in the glassy state decreased gradually. In the glassy state, the CTE of the 10 Å model was reduced by 5.70% compared to that of the 6.5 Å system and 7.70% compared to that of the pure EP; while the CTE in the rubbery state increased with the particle size. In general, the CTE in the glassy state provided a better referential value considering the fact that the actual working state of the EP materials was the glassy state.

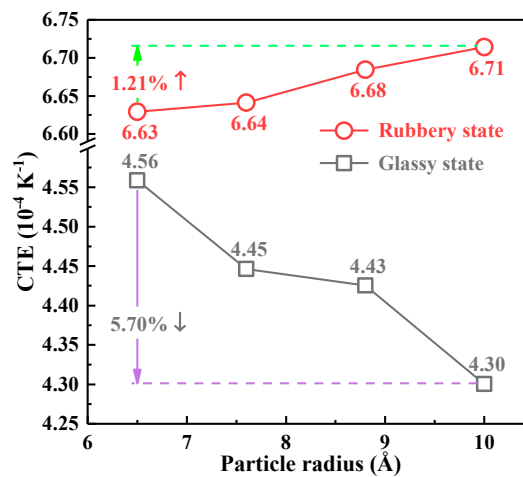


Figure 9. The CTE with different particle sizes under 67% crosslinking density.

3.5. Elastic Moduli

The static constant strain method [44] was used to analyze the mechanical properties of the EP systems in this paper. A slight strain was applied to the system, which was originally in the state of mechanical equilibrium, to enable the model to generate the uniaxial tension and compression deformation along the x-, y- and z-axis, respectively, i.e., shear deformation in the xy-, xz- and yz-plane, correspondingly. The stress-strain relationship obeys Hooke’s law:

$$\sigma = C\varepsilon \tag{5}$$

where σ is the stress vector, ϵ is strain vector and C is the stiffness matrix. The EP models in the simulation can be regarded as an isotropic material; thus, C can be simplified as follows:

$$\begin{bmatrix} \lambda + 2\mu & 0 & 0 & 0 & 0 & 0 \\ 0 & \lambda + 2\mu & 0 & 0 & 0 & 0 \\ 0 & 0 & \lambda + 2\mu & 0 & 0 & 0 \\ 0 & 0 & 0 & \mu & 0 & 0 \\ 0 & 0 & 0 & 0 & \mu & 0 \\ 0 & 0 & 0 & 0 & 0 & \mu \end{bmatrix} \quad (6)$$

where λ and μ are elastic constants and can be obtained from the stiffness matrix. The parameters such as Young’s modulus E and shear modulus G of an EP system can be obtained from λ and μ :

$$E = \mu \frac{3\lambda + 2\mu}{\lambda + \mu} \quad (7)$$

$$G = \mu \quad (8)$$

The static mechanical properties of the pure EP and composites were investigated at 300 K. Figure 10 shows Young’s modulus and the shear modulus of pure EP and 6.5 Å composites. With the increase of the crosslinking density, the two modulus values increased for all systems. The reason is that the stable 3D polymer network structure formed by the curing agent, EP matrix and nano-SiO₂ further enhanced the stiffness and mechanical properties of the material. Furthermore, according to the results shown in Figure 8, the crosslinked structure lowered MSD and limited the molecular motion in the model, which may result in higher moduli, as well [38]. Moreover, the static mechanical properties of the nanocomposite systems were obviously better than that of the pure EP system, and the modulus growth rates with the crosslinking density of the composites were higher than that of pure EP. The main reason is the high module of nanoparticles, strengthening the epoxy matrix [7].

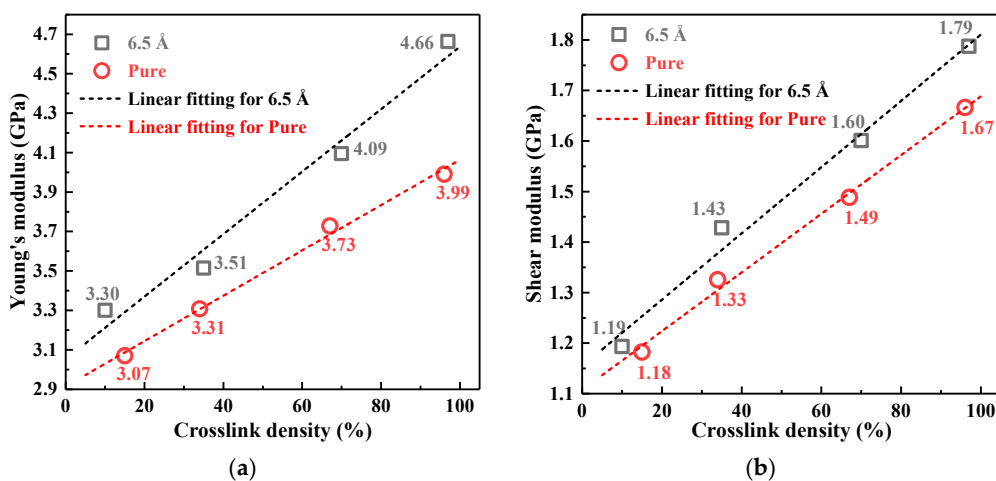


Figure 10. The static mechanical properties of the pure EP and 6.5 Å composites with different crosslinking densities. (a) Young’s modulus; (b) shear modulus.

The Young’s and shear moduli of the pure EP and composites with different particle sizes at a crosslinking density of 67% are shown in Figure 11. The doping of nano-SiO₂ with different particle sizes improved the mechanical properties of the DGEBA/MTHPA matrix to varying degrees. Among them, the 7.6 Å SiO₂ had the best performance, where Young’s modulus and the shear modulus increased by 12.60% and 8.72%, respectively. The phenomena were basically consistent with the results of free volume analysis. The smaller the particle size was, the smaller the free volume was, the higher

the moduli could be. However, when the particle size of SiO₂ was less than 7.6 Å, the Young's modulus and the shear modulus decreased slightly, which indicated that there were many factors affecting the mechanical properties of the nanocomposites. The interface characteristics produced by different particle sizes may be another factor affecting the mechanical properties, except the free volume.

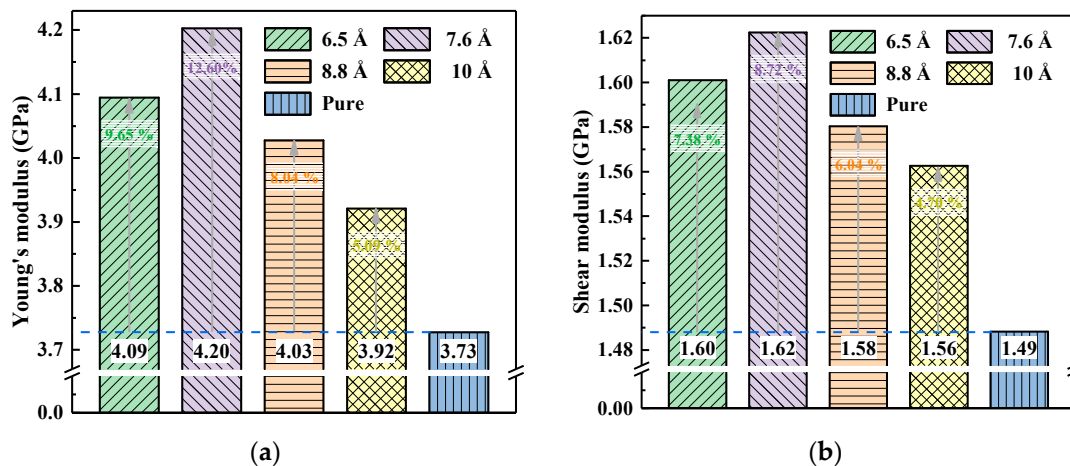


Figure 11. The static mechanical properties of the pure EP and composites with different particle sizes at a crosslinking density of 67%. (a) Young's modulus; (b) shear modulus.

4. Conclusions

In this paper, an automatic crosslinking method for epoxy resin, anhydride curing agent and nano-SiO₂ was developed, which effectively improved the accuracy of modeling and the molecular simulation efficiency of epoxy composites. The microstructure, thermal and mechanical properties of epoxy resin and its composites were studied by molecular dynamics. The results show that the crosslinking densities of epoxy resin and the doping of nano-SiO₂ can influence the structure and properties of the materials in many ways. The obtained findings are as follows:

1. The thermal and mechanical properties were improved by increasing the crosslinking density. With the increase of crosslinking density, the glass transition temperature (T_g) increased and the coefficient of thermal expansion (CTE) decreased; in addition, Young's modulus and the shear modulus of the materials increased, and the mechanical properties were enhanced.
2. Doping nano-SiO₂ particles into epoxy resin effectively improved the thermal and mechanical properties, and the effectiveness was closely related to the particle size of nano-SiO₂. The T_g value increased with the decreasing particle size. Compared with pure epoxy resin, the T_g of 6.5 Å composite model was increased by 6.68%. The variation of CTE in the glassy state demonstrated opposite trend as compared with T_g value. The CTE of 10 Å composite model was the lowest, which is 7.70% less than that of pure epoxy. In addition, the mechanical properties first increased and then decreased with the decreasing particle size. Both the Young's modulus and shear modulus reached the maximum at the 7.6 Å, and increased by 12.60% and 8.72% respectively compared with pure epoxy.
3. The thermal and mechanical properties are closely related to the Fraction of Free Volume (FFV) and Mean Squared Displacement (MSD). The crosslinking process and the nano-SiO₂ doping reduced the FFV in the model, impeded the deformation and improved the elastic modulus of the system. Moreover, the decreasing FFV reduced the MSD of the model, limited the segment motion of the molecular chains and made it even harder for the glass transition.

Author Contributions: Q.X., X.Y., F.L. and K.F. conceived of and designed the simulations. L.L. and S.L. performed the MD simulations. Q.X. and K.F. analyzed the data. Z.H. contributed the analysis tools. L.L. and B.L. wrote the paper.

Funding: This research was funded by the National Key R&D Program of China (Grant No. 2017YFB0903800), the Fundamental Research Funds for the Central Universities (Grant No. 2016ZZD07), and the Technology Foundation of SGCC (PGKJ2018-151).

Conflicts of Interest: The authors declare no conflict of interest.

References

1. Xie, Q.; Lin, H.F.; Zhang, S.; Wang, R.X.; Kong, F.; Shao, T. Deposition of $\text{SiC}_x\text{H}_y\text{O}_z$ thin film on epoxy resin by nanosecond pulsed appj for improving the surface insulating performance. *Plasma Sci. Technol.* **2018**, *20*. [[CrossRef](#)]
2. He, X.; Xu, X.; Wan, Q.; Bo, G.; Yan, Y. Synthesis and characterization of dimmer-acid-based nonisocyanate polyurethane and epoxy resin composite. *Polymers* **2017**, *9*, 649. [[CrossRef](#)]
3. Kumar, S.; Krishnan, S.; Samal, S.K.; Mohanty, S.; Nayak, S.K. Toughening of petroleum based (DGEBA) epoxy resins with various renewable resources based flexible chains for high performance applications: A review. *Ind. Eng. Chem. Res.* **2018**, *57*, 2711–2726. [[CrossRef](#)]
4. Zhou, X.; Qiu, S.; Xing, W.; Gangireddy, C.S.R.; Gui, Z.; Hu, Y. Hierarchical polyphosphazene@molybdenum disulfide hybrid structure for enhancing the flame retardancy and mechanical property of epoxy resins. *ACS Appl. Mater. Interfaces* **2017**, *9*, 29147–29156. [[CrossRef](#)] [[PubMed](#)]
5. Bobby, S.; Samad, M.A. Enhancement of tribological performance of epoxy bulk composites and composite coatings using micro/nano fillers: A review. *Polym. Adv. Technol.* **2017**, *28*, 633–644. [[CrossRef](#)]
6. Zabihi, O.; Ahmadi, M.; Nikafshar, S.; Chandrakumar Preyeswary, K.; Naebe, M. A technical review on epoxy-clay nanocomposites: Structure, properties, and their applications in fiber reinforced composites. *Compos. Part B Eng.* **2018**, *135*, 1–24. [[CrossRef](#)]
7. Nikje, M.M.A.; Garmarudi, A.B.; Tehrani, Z.M.; Haghshenas, M.; Shakhesi, S. Thermal and mechanical evaluation of epoxy resin composites by synthesis of amine-based coupling agent-nano silica complex. *Polym.-Plast. Technol.* **2011**, *50*, 646–650. [[CrossRef](#)]
8. Faridirad, F.; Ahmadi, S.; Barmar, M. Polyamide/carbon nanoparticles nanocomposites: A review. *Polym. Eng. Sci.* **2017**, *57*, 475–494. [[CrossRef](#)]
9. Hoyos, M.; García, N.; Navarro, R.; Dardano, A.; Ratto, A.; Guastavino, F.; Tiemblo, P. Electrical strength in ramp voltage ac tests of ldpe and its nanocomposites with silica and fibrous and laminar silicates. *J. Polym. Sci. Pol. Phys.* **2008**, *46*, 1301–1311. [[CrossRef](#)]
10. Njuguna, J.; Pielichowski, K.; Desai, S. Nanofiller-reinforced polymer nanocomposites. *Polym. Adv. Technol.* **2008**, *19*, 947–959. [[CrossRef](#)]
11. Shao, T.; Liu, F.; Hai, B.; Ma, Y.F.; Wang, R.X.; Ren, C.Y. Surface modification of epoxy using an atmospheric pressure dielectric barrier discharge to accelerate surface charge dissipation. *IEEE Trans. Dielectr. Electr. Insul.* **2017**, *24*, 1557–1565. [[CrossRef](#)]
12. Mo, H.; Huang, X.; Liu, F.; Yang, K.; Li, S.; Jiang, P. Nanostructured electrical insulating epoxy thermosets with high thermal conductivity, high thermal stability, high glass transition temperatures and excellent dielectric properties. *IEEE Trans. Dielectr. Electr. Insul.* **2015**, *22*, 906–915. [[CrossRef](#)]
13. Yang, L.; Qi, C.; Wu, G.; Liao, R.; Wang, Q.; Gong, C.; Gao, J. Molecular dynamics simulation of diffusion behaviour of gas molecules within oil-paper insulation system. *Mol. Simul.* **2013**, *39*, 988–999. [[CrossRef](#)]
14. Verma, A.; Parashar, A.; Packirisamy, M. Atomistic modeling of graphene/hexagonal boron nitride polymer nanocomposites: A review. *WIREs Comput. Mol. Sci.* **2018**, *8*, e1346. [[CrossRef](#)]
15. Paquet, E.; Viktor, H.L. Molecular dynamics, monte carlo simulations, and langevin dynamics: A computational review. *BioMed Res. Int.* **2015**, *2015*, 183918. [[CrossRef](#)] [[PubMed](#)]
16. Masoumi, S.; Arab, B.; Valipour, H. A study of thermo-mechanical properties of the cross-linked epoxy: An atomistic simulation. *Polymer* **2015**, *70*, 351–360. [[CrossRef](#)]
17. Li, K.; Li, Y.; Lian, Q.; Cheng, J.; Zhang, J. Influence of cross-linking density on the structure and properties of the interphase within supported ultrathin epoxy films. *J. Mater. Sci.* **2016**, *51*, 9019–9030. [[CrossRef](#)]
18. Odegard, G.M.; Jensen, B.D.; Gowtham, S.; Wu, J.; He, J.; Zhang, Z. Predicting mechanical response of crosslinked epoxy using reaxff. *Chem. Phys. Lett.* **2014**, *591*, 175–178. [[CrossRef](#)]
19. Sirk, T.W.; Khare, K.S.; Karim, M.; Lenhart, J.L.; Andzelm, J.W.; McKenna, G.B.; Khare, R. High strain rate mechanical properties of a cross-linked epoxy across the glass transition. *Polymer* **2013**, *54*, 7048–7057. [[CrossRef](#)]

20. Zhang, X.; Wen, H.; Wu, Y. Computational thermomechanical properties of silica–epoxy nanocomposites by molecular dynamic simulation. *Polymers* **2017**, *9*, 430. [[CrossRef](#)]
21. Choi, J.; Yu, S.; Yang, S.; Cho, M. The glass transition and thermoelastic behavior of epoxy-based nanocomposites: A molecular dynamics study. *Polymer* **2011**, *52*, 5197–5203. [[CrossRef](#)]
22. Chen, S.; Sun, S.; Steven, G.; Li, C.; Wang, X.; Hu, S. Molecular dynamics simulations of the interaction between carbon nanofiber and epoxy resin monomers. *Acta Polym. Sin.* **2015**, 1158–1164. (In Chinese) [[CrossRef](#)]
23. Zhu, R.; Pan, E.; Roy, A.K. Molecular dynamics study of the stress–strain behavior of carbon-nanotube reinforced epon 862 composites. *Mater. Sci. Eng. A Struct.* **2007**, *447*, 51–57. [[CrossRef](#)]
24. Zheng, Y.; Chonung, K.; Wang, G.; Wei, P.; Jiang, P. Epoxy/nano-silica composites: Curing kinetics, glass transition temperatures, dielectric, and thermal-mechanical performances. *J. Appl. Polym. Sci.* **2009**, *111*, 917–927. [[CrossRef](#)]
25. Li, W.; Feng, W.; Huang, H. High-performance epoxy resin/silica coated flake graphite composites for thermal conductivity and electrical insulation. *J. Mater. Sci. Mater. Electron.* **2016**, *27*, 6364–6370. [[CrossRef](#)]
26. Hsieh, T.H.; Kinloch, A.J.; Masania, K.; Taylor, A.C.; Sprenger, S. The mechanisms and mechanics of the toughening of epoxy polymers modified with silica nanoparticles. *Polymer* **2010**, *51*, 6284–6294. [[CrossRef](#)]
27. Liu, F.; Wang, Z.Q.; Liang, W.Y.; Qu, Y.W. Effect of nano-silica on flexural properties of epoxy resin. *Adv. Mater. Res.* **2011**, 383–390, 3845–3848. [[CrossRef](#)]
28. Lee, D.H.; Lee, N.; Park, H. Role of silica nanoparticle in multi-component epoxy composites for electrical insulation with high thermal conductivity. *J. Am. Ceram. Soc.* **2018**, *101*, 2450–2458. [[CrossRef](#)]
29. Park, J.-J.; Lee, J.-Y. Effect of epoxy-modified silicone-treated micro-/nano-silicas on the electrical breakdown strength of epoxy/silica composites. *IEEE Trans. Dielectr. Electr. Insul.* **2017**, *24*, 3794–3800. [[CrossRef](#)]
30. Li, Y.; Tian, M.; Lei, Z.; Zhang, J. Effect of nano-silica on dielectric properties and space charge behavior of epoxy resin under temperature gradient. *J. Phys. D Appl. Phys.* **2018**, *51*, 12530912. [[CrossRef](#)]
31. He, J.M.; Huang, Y.D. Effect of silane-coupling agents on interfacial properties of CF/PI composites. *J. Appl. Polym. Sci.* **2007**, *106*, 2231–2237. [[CrossRef](#)]
32. Zhang, X.; Chen, X.; Xiao, S.; Wen, H.; Wu, Y. Molecular Dynamics Simulation of Thermal-mechanical Properties of Modified SiO₂ Reinforced Epoxy Resin. *High Volt. Eng.* **2018**, *44*, 740–749. (In Chinese) [[CrossRef](#)]
33. Wu, C.; Xu, W. Atomistic molecular modelling of crosslinked epoxy resin. *Polymer* **2006**, *47*, 6004–6009. [[CrossRef](#)]
34. Lu, Y.-Y.; Shu, Y.-J.; Liu, N.; Shu, Y.; Wang, K.; Wu, Z.-K.; Wang, X.-C.; Ding, X.-Y. Theoretical simulations on the glass transition temperatures and mechanical properties of modified glycidyl azide polymer. *Comput. Mater. Sci.* **2017**, *139*, 132–139. [[CrossRef](#)]
35. Wei, Q.; Zhang, Y.; Wang, Y.; Yang, M. A molecular dynamic simulation method to elucidate the interaction mechanism of nano-SiO₂ in polymer blends. *J. Mater. Sci.* **2017**, *52*, 12889–12901. [[CrossRef](#)]
36. Huang, Y.Z.; Tian, Y.Z.; Li, Y.Y.; Tan, X.C.; Li, Q.; Cheng, J.; Zhang, J.Y. High mechanical properties of epoxy networks with dangling chains and tunable microphase separation structure. *RSC Adv.* **2017**, *7*, 49074–49082. [[CrossRef](#)]
37. Kojio, K.; Furukawa, M.; Matsumura, S.; Motokucho, S.; Osajima, T.; Yoshinaga, K. The effect of cross-linking density and dangling chains on surface molecular mobility of network polyurethanes. *Polym. Chem. UK* **2012**, *3*, 2287–2292. [[CrossRef](#)]
38. Asaad, J.; Gomaa, E.; Bishay, I.K. Free-volume properties of epoxy composites and its relation to macrostructure properties. *Mater. Sci. Eng. A Struct.* **2008**, *490*, 151–156. [[CrossRef](#)]
39. Zhang, W.; Qing, Y.; Zhong, W.; Sui, G.; Yang, X. Mechanism of modulus improvement for epoxy resin matrices: A molecular dynamics simulation. *React. Funct. Polym.* **2017**, *111*, 60–67. [[CrossRef](#)]
40. Wang, Y.-H.; Wang, W.-H.; Zhang, Z.; Xu, L.; Li, P. Study of the glass transition temperature and the mechanical properties of pet/modified silica nanocomposite by molecular dynamics simulation. *Eur. Polym. J.* **2016**, *75*, 36–45. [[CrossRef](#)]
41. Chinkanjanarot, S.; Radue, M.S.; Gowtham, S.; Tomasi, J.M.; Klimek-McDonald, D.R.; King, J.A.; Odegard, G.M. Multiscale thermal modeling of cured cycloaliphatic epoxy/carbon fiber composites. *J. Appl. Polym. Sci.* **2018**, *135*. [[CrossRef](#)]
42. Xue, Q.; Lv, C.; Shan, M.; Zhang, H.; Ling, C.; Zhou, X.; Jiao, Z. Glass transition temperature of functionalized graphene–polymer composites. *Comput. Mater. Sci.* **2013**, *71*, 66–71. [[CrossRef](#)]

43. Lin, S.; Huang, Y.; Xie, D.; Min, D.; Wang, W.; Yang, L.; Li, S. Molecular relaxation and glass transition properties of epoxy resin at high temperature. *Acta Phys. Sin.* **2016**, *65*, 304–310. (In Chinese) [[CrossRef](#)]
44. Shokuhfar, A.; Arab, B. The effect of cross linking density on the mechanical properties and structure of the epoxy polymers: Molecular dynamics simulation. *J. Mol. Model.* **2013**, *19*, 3719–3731. [[CrossRef](#)] [[PubMed](#)]



© 2018 by the authors. Licensee MDPI, Basel, Switzerland. This article is an open access article distributed under the terms and conditions of the Creative Commons Attribution (CC BY) license (<http://creativecommons.org/licenses/by/4.0/>).